Available online at www.sciencedirect.com
ScienceDirect
Catalysis Today 125 (2007) 137–142
CATALYSIS TODAY
www.elsevier.com/locate/cattod

A new route to prepare supported nickel phosphide/silica–alumina hydrotreating catalysts from amorphous alloys

Limin Song [a,b], Wei Li [a,*], Guanglei Wang [a], Minghui Zhang [a], Keyi Tao [a]

[a] *Institute of New Catalytic Materials Science, College of Chemistry, Nankai University, Tianjin 300071, PR China*
[b] *College of Material Science and Chemical Engineering, Tianjin Polytechnic University, Tianjin 300160, PR China*

Available online 8 April 2007

Abstract

Supported nickel phosphides were prepared by treating an amorphous Ni–B alloy on silica–alumina support with phosphine (15 vol.% PH_3/H_2) at relatively low temperature. The amorphous Ni–B/SiO_2–Al_2O_3 precursors were synthesized by silver-induced electroless plating. The amorphous precursors and catalysts were characterized by X-ray diffraction, high-resolution transmission electron microscopy, selected area electron diffraction, BET surface area and inductively coupled plasma measurements. The transmission electron micrographs of the Ni_2P/SiO_2–Al_2O_3 particles with their size ranging from 60 to 80 nm showed that they were homogeneously dispersed over the SiO_2–Al_2O_3 support. The as-prepared catalysts exhibited an excellent catalytic activity in the hydrodesulfurization (HDS) of dibenzothiophene.

Keywords: Amorphous alloy; Silver-induced electroless plating; Nickel phosphide; Phosphine; Hydrodesulfurization; Silica–alumina; Dibenzothiophene

1. Introduction

The need to produce a cleaner environment has resulted in a global tightening in the allowed sulfur content of fuels. Many countries have issued new legislations to lower the allowed content in diesel fuel from the current 500–15 ppmW, and in gasoline from 300 to 30 ppmW. Therefore, hydrodesulfurization (HDS) and hydrodenitrogenation (HDN) of low-quality petroleum feedstock become increasingly important. For this reason, considerable efforts have been made being expended over the past decade to develop high-performance HDS catalysts. Many researchers modified the classic alumina-supported Mo or W sulfide catalysts promoted with Ni or Co, or investigated new active phases such as metal carbides and nitrides [1–8]. Transition-metal phosphides as a new class of hydrotreating catalysts have also attracted considerable attention. Many groups have investigated the hydrotreating of petroleum feedstocks using transition-metal phosphides, and found that these catalysts showed high activity and selectivity in HDS [9–13]. In particular, Ni_2P was found to be the most active phase among these phosphides, although other phosphides such as MoP and WP showed high HDS activities as well. Traditional supported metal phosphides were prepared by the temperature programmed reduction (TPR) method, by which the metal salt was heated together with ammonium phosphate in hydrogen. The method is simple and easy to operate. However, it requires high temperature and easily produces impurities. Other methods, such as the solvothermal method [14], the thermal decomposition of metal–phosphine complexes [15], and the thermal decomposition of single-source molecular precursors [16], have been reported in the past years. All these methods are very useful and important, but are unsuitable for the synthesis of supported metal phosphide catalysts. Therefore, it is significant to develop an easy and effective synthesis method for preparing supported metal phosphides at low temperatures.

In the past decade, amorphous alloys have gained increasing attention as novel catalytic materials [17–20], for their unique combination of small particle size and short-range ordering as well as long-range disordered structure. Our group has carried out extensive researches in this area [21–23]. Apart from their good catalytic performance, amorphous alloys can be easily transformed into the corresponding nanocrystalline materials (NC) under proper treatment conditions, due to the metastable structure of the nanoscaled amorphous alloys [24,25]. In recent years, the amorphous-to-NC process has been thoroughly investigated and successfully applied to obtain NC materials in

* Corresponding author. Tel.: +86 22 23508662; fax: +86 22 23508662.
E-mail address: weili@nankai.edu.cn (W. Li).

0920-5861/$ – see front matter © 2007 Elsevier B.V. All rights reserved.
doi:10.1016/j.cattod.2007.02.033

various systems [26–32]. In terms of this characteristic of amorphous alloys, in this paper, we report on a new route to preparing Ni_2P/SiO_2–Al_2O_3 by treating amorphous Ni–B alloys with PH_3 at low temperature. In general, it is very important to control the dispersion of the active sites on the surface. Therefore, we choose the metal-induced electroless-plating route from the numerous methods for synthesizing amorphous alloy precursors, so that amorphous particles can be first anchored to and homogeneously dispersed over the support, which favours to producing a supported Ni_2P catalyst with high dispersion. Recently, Yang et al. have reported a method to prepare Ni_2P/SiO_2 by treating Ni/SiO_2 with PH_3 [33]. The preparation conditions were mild. However, they only used silica as the carrier. Here, we use industrial amorphous silica–alumina (silica 88 wt.%, alumina 12 wt.%) as a carrier because it provides much higher surface area and large pores enough to assure a high dispersion of the active phase on the support. To avoid a strong interaction induced by a high reduction temperature between nickel phosphide and the surface of the support, we use the electroless-plating method and first plate a Ni-based alloy on the support at 35 °C, and subsequently treat the amorphous alloy at a relatively low temperature.

2. Experimental

2.1. Preparation of amorphous alloy precursors

Commercially available solvents and reagents were used without further purification. The Ni–B/SiO_2–Al_2O_3 amorphous alloy precursors were prepared by the silver-induced electroless-plating method [23]. Silver nitrate (0.02 g) was dissolved in distilled water (47.5 mL), silica–alumina (10.0 g) was added to, and then the solution was stirred for 3.0 h. The resulting Ag/SiO_2–Al_2O_3 was filtered, washed with a small volume of distilled water and dried under vacuum at 120 °C for 3 h. The Ni–B plating solution consisted of nickel sulfate (7.9 g/L), ammonium hydroxide (15 g/L), and potassium borohydride (5.5 g/L). The required amount of Ag/SiO_2–Al_2O_3 was added to 100 mL of the plating solution. The resulting solution was heated to 35 °C and vigorously stirred. After 0.5 h, the black Ni–B/Ag/SiO_2–Al_2O_3 precipitate was collected, washed with a small volume of distilled water and anhydrous ethanol, and then dried under vacuum at 80 °C for 3 h.

2.2. Catalyst preparation

The resulting Ni–B/Ag/SiO_2–Al_2O_3 was heated at 150–350 °C in a sealed quartz tube in a furnace, and 15 vol.% PH_3/H_2 (synthesized using the procedure given in [34]) carried by hydrogen was passed through the quartz tube at a rate of 5 mL min^{-1}. The reaction was maintained for 2 h, and then the sample was cooled to room temperature in flowing argon. Finally, the samples were passivated in a flow of 1 vol.% O_2/N_2 (10 mL/min). The passivated samples were handled in air.

2.3. Amorphous precursor and catalyst characterization

The particle size and surface morphology of the samples were determined using a JEOL-2010 high-resolution transmission electron microscope (HRTEM) equipped with a selected area electron diffraction (SAED) system. The X-ray diffraction (XRD) patterns of the samples were recorded on a Rigaku-D/MAX 2500 X-ray powder diffractometer with a Cu Kα radiation source (λ = 1.5418 Å). A scan rate of 0.05° s^{-1} was used to record the patterns in the 2θ range 20–80°. The elemental content of the samples was determined using the inductively coupled plasma (ICP-AES, 9000(N + M)) method. The BET surface areas (S_{BET}) were measured by N_2 adsorption at −196 °C using an automatic surface area and pore size analyzer (Autosorb-1-MP 1530VP). S_{BET} measurements were performed using the five-point BET method.

2.4. Activity test

The HDS of dibenzothiophene was carried out in a flowing fixed-bed reactor using a feed consisting of a decalin solution of DBT (0.5 wt.%). The conditions of the HDS reaction were 320 °C, 3.0 MPa, WHSV = 9 h^{-1}, and H_2 flow rate 90 ml min^{-1}. 1.0 mL (0.6 g) of Ni_2P/SiO_2–Al_2O_3 catalyst diluted with quartz sands to 5.0 mL was reduced by heating from room temperature to a certain temperature in H_2 (200 mL min^{-1}), maintaining the sample at that temperature for 2 h, before changing the temperature to the desired reaction temperature. Liquid samples were collected every hour and analyzed by a gas chromatography with a flame ionization detector (FID) and a capillary column (OV101). The DBT conversion was used as a measure of the HDS activity.

3. Results and discussion

3.1. Characterization of the amorphous precursors and catalysts

All supported catalysts were prepared with the same loading of nickel (Table 1). Fig. 1 shows the XRD patterns of the amorphous samples and the SiO_2–Al_2O_3 support. The XRD pattern of the support shows that the SiO_2–Al_2O_3 powder is amorphous, because of the lack of sharp peaks. The XRD

Table 1
Compositions and specific areas of the Ni–B/Ag/SiO_2–Al_2O_3 precursors and Ni_2P/Ag/SiO_2–Al_2O_3 catalysts

Sample	Metal loading (wt.%)	S_{BET}/m^2 g^{-1}	Composition (atomic ratio)	Content of B (wt.%)	Content of Ag (wt.%)
Ag/SiO_2–Al_2O_3	–	–	–	–	0.16
Ni–B/SiO_2–Al_2O_3	10.93 (Ni)	221	$Ni_{75.2}B_{24.8}$	0.62	0.16
Ni_2P/SiO_2–Al_2O_3	10.93 (Ni)	142	$Ni_{2.06}P$	0.59	0.15

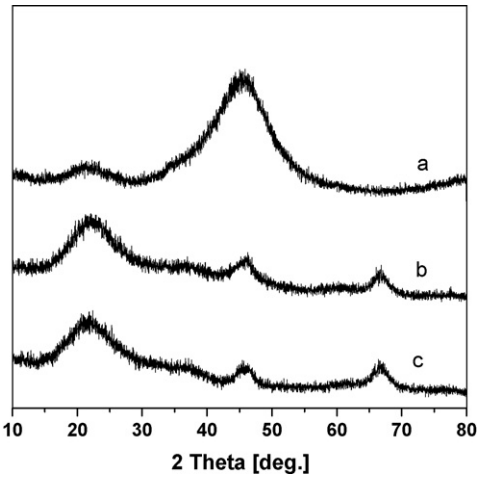

Fig. 1. XRD patterns of (a) amorphous Ni–B, (b) amorphous Ni–B/SiO_2–Al_2O_3, and (c) SiO_2–Al_2O_3.

patterns of the Ni–B alloy and Ni–B/SiO_2–Al_2O_3 catalyst are presented in Fig. 1a and b. The broad and dispersive peak at $2\theta = 45^\circ$ is caused by the amorphous structure of the Ni–B particles and is characteristic to amorphous alloy (Fig. 1a). The small profile around $2\theta = 22^\circ$ is attributed to amorphous boron oxide, which is inevitably formed when the reduction is carried out in aqueous solution [35]. The Ni–B/SiO_2–Al_2O_3 sample does not show obvious differences from the SiO_2–Al_2O_3 carrier (Fig. 1b) due to the very good dispersion of the Ni–B particles on the support. In addition, the strong peak of the support around $2\theta = 45^\circ$ and the weak diffraction signal of amorphous Ni–B alloy cannot be neglected.

The XRD patterns of the samples treated by PH_3 at 150–350 °C are shown in Fig. 2b–f. The samples obtained at 150, 200, 250, 300 and 350 °C are denoted as Ni_2P-150, Ni_2P-200, Ni_2P-250, Ni_2P-300, and Ni_2P-350, respectively. The sharp diffraction lines (around $2\theta = 40.8$, 44.6, and 47.3°) of the five samples are assigned to the hexagonal cell of the Ni_2P phase. The XRD pattern of Ni_2P is similar to the reference pattern taken from the JCPDS powder diffraction file (Card 65-1989) [36], as well as the XRD patterns of Ni_2P reported recently by others [9–13]. It can be observed that there are no crystalline impurities other than the phase of Ni_2P in Fig. 2b–f. However, whether the amorphous structure has disappeared with increasing reaction temperature cannot be concluded from the XRD patterns of the samples, because the $2\theta = 45^\circ$ peak of Ni–B overlaps with the peak of silica–alumina. Bulk Ni–B was only completely converted to crysatalline Ni_2P at 250 °C, because the dispersive characteristic peak of the amorphous alloy at $2\theta = 45^\circ$ just disappeared until 250 °C in the XRD pattern of bulk Ni_2P (Fig. 3). Therefore, we concluded that the amorphous characteristic of the samples had not disappeared at 150 and 200 °C, and that all the diffraction lines were due to crystalline Ni_2P and the SiO_2–Al_2O_3 support when the reaction temperature was further increased to 250, 300 and 350 °C (Fig. 2d–f). However, the intensity of the Ni_2P peaks first increased gradually and then decreased from 250 to 350 °C. The reason is the better crystallization of the Ni_2P at higher temperature. The narrower peak width also proves the point with the increasing temperature. The decreased intensity at 350 °C may be ascribed to the interaction between the Ni_2P phase and the support [37]. These experimental results demonstrate that the treatment temperature is a key factor in determining the reaction products. In addition, the traditional temperature-programmed reduction (TPR) method must break the strong P–O bond in phosphates [33]. Therefore, the route requires a high temperature. In comparison with the TPR method, we utilize the reaction of metastable and nanoscale amorphous alloys with PH_3, so that the catalysts can be prepared under mild conditions. The representative nickel phosphide catalysts were prepared at 250 °C, which guarantees that the amorphous precursors could be completely transformed.

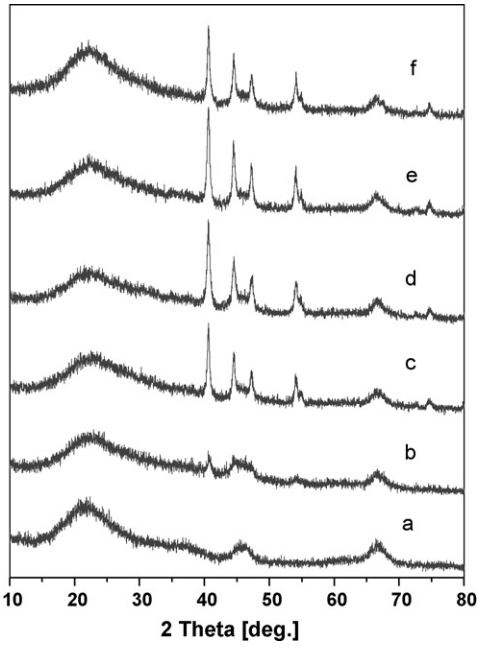

Fig. 2. XRD patterns of (a) SiO_2–Al_2O_3, (b) Ni_2P-150, (c) Ni_2P-200, (d) Ni_2P-250, (e) Ni_2P-300, and (f) Ni_2P-350.

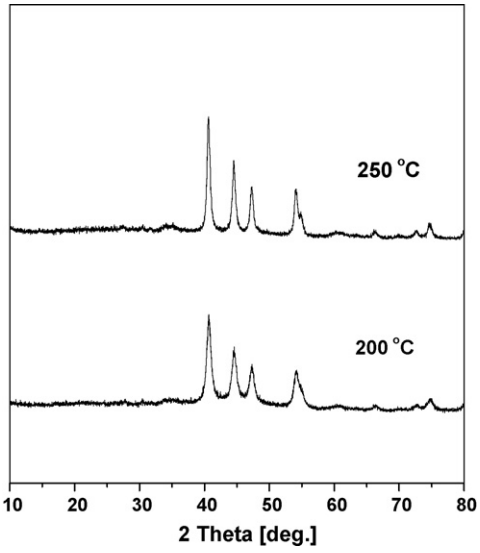

Fig. 3. XRD patterns of Ni_2P from bulk Ni–B.

The bulk compositions of the as-prepared samples determined by ICP analysis are given in Table 1. Table 1 shows that the chemical composition of supported Ni–B was $Ni_{75.2}P_{24.8}$. Table 1 also shows that the average mole ratio of nickel to phosphorus in the as-prepared supported Ni_2P samples is 2.06. In addition, as shown in Table 1, a small quantity of boron and silver still remains in the Ni_2P sample.

The TEM and HRTEM images of the as-synthesized Ni–B/SiO_2–Al_2O_3 and Ni_2P-250/SiO_2–Al_2O_3 samples are shown in Fig. 4. Fig. 4a shows that the spherical Ni–B particles with their diameters in the range of 40–60 nm were homogenously dispersed on the support. According to the literature [23], in the formation process of amorphous Ni–B, tiny silver clusters are first distributed randomly over the support; after several minutes, the silver clusters are coated with deposited nickel clusters due to

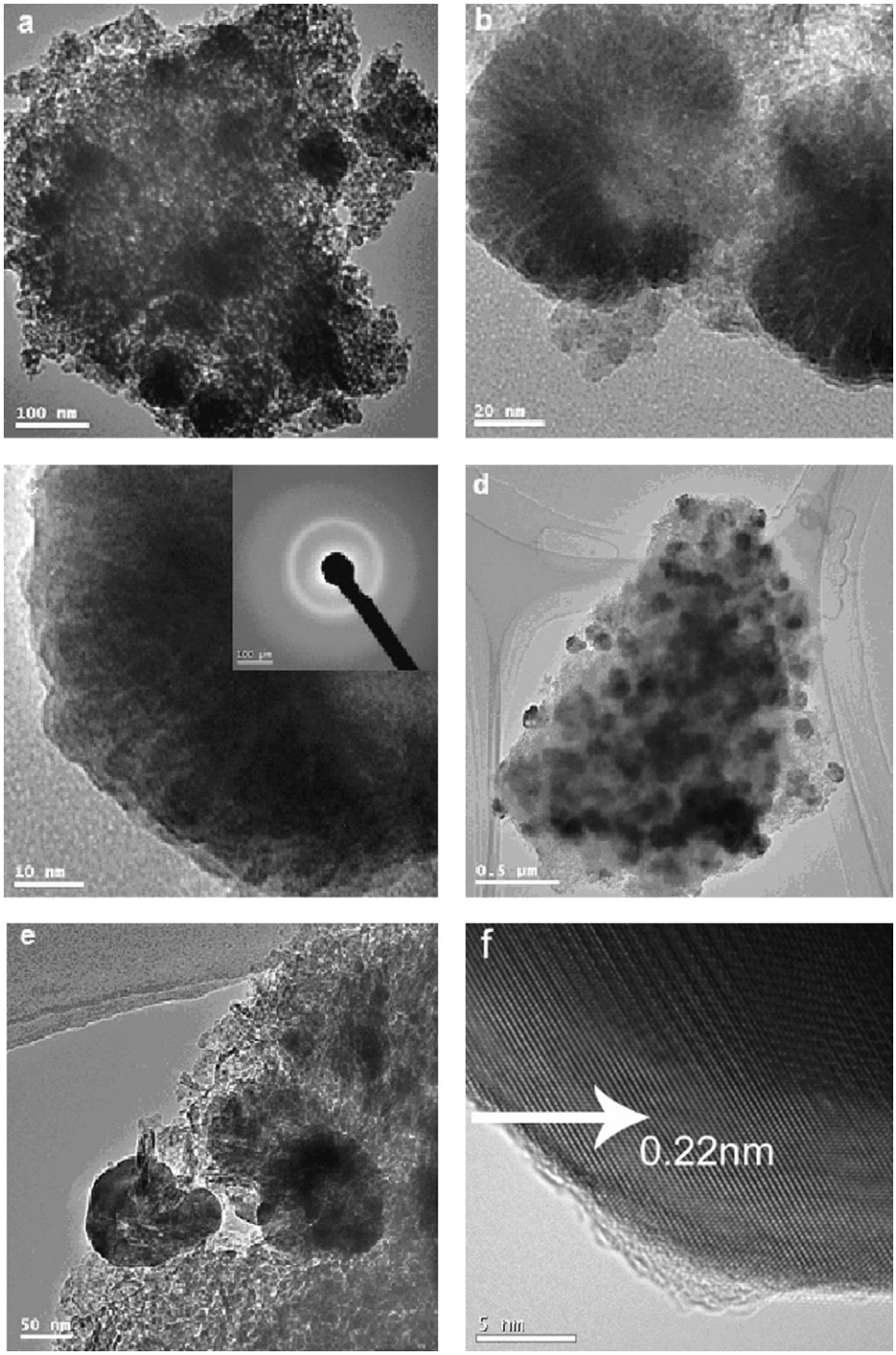

Fig. 4. TEM and HRTEM micrographs of (a) Ni–B/SiO_2–Al_2O_3, (b) Ni–B/SiO_2–Al_2O_3, (c) Ni–B/SiO_2–Al_2O_3, (d) Ni_2P-250/SiO_2–Al_2O_3, (e) Ni_2P-250/SiO_2–Al_2O_3, and (f) Ni_2P-250/SiO_2–Al_2O_3.

the silver catalysis. The results clearly show that silver plays an important role in controlling the dispersion of Ni–B on the support. By carefully observing Fig. 4b, we can see that every particle contains many regular pores from the interior to the exterior surface. It is obvious that the structure is different from the solid spheres of conventional Ni–B particles [22]. The reason for forming a porous structure is mainly due to the process of preparing the supported amorphous Ni–B by the silver-catalyzed chemical plating method [23]. The porous structure can expose more metal sites on the surface so that it is easier to form Ni_2P when Ni–B was treated by PH_3. To investigate the nature of Ni–B, a Ni–B particle was magnified further (Fig. 4c). Fig. 4c clearly shows there is no visible lattice in the particle, which is characteristic to an amorphous substance. The result is consistent with the XRD pattern (Fig. 1b). In addition, a dispersive ring in the SAED further testifies that the Ni–B sample is amorphous (Fig. 4c). Figs. 4d–f shows the TEM and HRTEM images of Ni_2P-250/SiO_2–Al_2O_3. The TEM image of the Ni_2P-250/SiO_2–Al_2O_3 sample (Fig. 4d) shows that the Ni_2P particles are spherical and homogenously dispersed over the support. The particle size is in the range of 60–80 nm (Fig. 4e). In the HRTEM image of the Ni_2P particles on the SiO_2–Al_2O_3 support (Fig. 4f), the visible lattice spacing is 0.22 nm, consistent with the d-spacing value for {1 1 1} crystallographic planes of the Ni_2P phase measured by XRD (Fig. 2d). This result further testifies that the active phase on the support is crystalline Ni_2P.

3.2. Activity measurements

The hydrotreating activity of the Ni_2P/SiO_2–Al_2O_3 catalysts was tested by the HDS of DBT. To further study the preparation of the SiO_2–Al_2O_3-supported catalysts, the effects of treatment temperature, carrier gas and reduction temperature on the HDS activity of the as-synthesized nickel phosphides were investigated. The Ni loading in all samples was 10.93 wt.% (Table 1). The specific areas are also listed in Table 1. As shown in Table 1, the specific area of Ni–B/SiO_2–Al_2O_3 is higher than that of Ni_2P/SiO_2–Al_2O_3. The decrease in the BET area is mainly caused by the pore blocking of the silica–alumina support.

Fig. 5 shows the effect of the final treatment temperature on the HDS performance of Ni_2P/SiO_2–Al_2O_3. It is obvious that the active phase can be obtained above 250 °C, in agreement with the XRD analysis results. The Ni–B on the support was not completely transformed to the active Ni_2P phase at 150 and 200 °C, and the structure of crystalline Ni_2P was not well formed because the diffraction line intensity of the products is very faint at 150 and 200 °C (Fig. 2b and c), therefore the two samples exhibit a decreasing HDS activity with time on stream (Fig. 5a and b). The conversion of DBT reached 100% and the activity maintains stable when the treatment temperature was increased to 250 and 300 °C (Fig. 5c and d). It is clear that the treatment at 250 and 300 °C gave much better results than that at other temperatures. However, the conversion fell to 89% when the treatment temperature reached 350 °C (Fig. 5e). A possible reason for this is the effect of the interaction between the Ni_2P phase and the support. The interaction results in a lower content of Ni_2P, so that the HDS activity decreases. Therefore, it is suggested that the treatment at 250 or 300 °C is necessary to prepare highly active nickel phosphides.

To investigate the effect of H_2 in the preparation process, H_2 was replaced by Ar. Fig. 6 shows that the gas type has significant on the HDS activity of the catalysts, demonstrating that the gas is not only a carrier or simply removes some adsorbents from the surface, but also may affect the optimization of the structure of phosphide. Therefore, it is clear that a mixture of H_2 and PH_3 is essential to obtain high-performance nickel phosphides in our method.

Generally, the catalysts were passivated with 1 vol.% O_2/N_2 before being exposed to air to prevent a rigorous breakage on the surface. But there is still a small oxide layer on the surface of the catalysts after passivation so that the performance of the catalysts will be greatly affected. Therefore, prior to the activity evaluation, the samples were reactivated in a H_2 flow. To investigate the effect of reduction temperature, the catalysts were evaluated after being reduced at 400 or 500 °C for 3 h. The HDS activity of the catalyst reached 100% when the reduction temperature was 400 °C and the WHSV was 9 h^{-1} (Fig. 7). Therefore, the WHSV was increased to 12 h^{-1} for the convenience of comparison. The results are displayed in Fig. 6. It is clear that the HDS conversion at 500 °C is superior to that at 400 °C. A possible reason for this is that the oxidized crystal structure is better renewed at the higher reduction

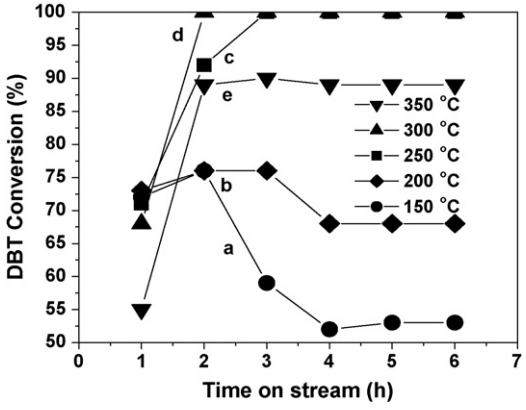

Fig. 5. Dependence of HDS activity on the final treatment temperature: (a) 150 °C, (b) 200 °C, (c) 250 °C, (d) 300 °C, and (e) 350 °C.

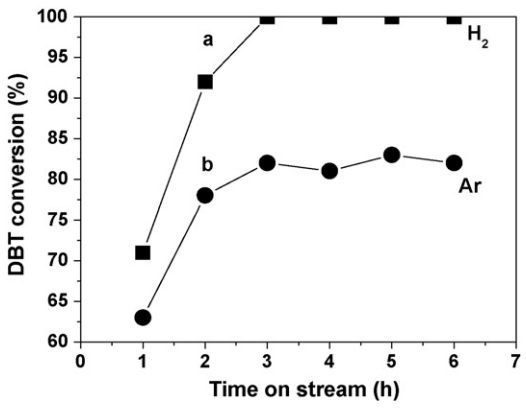

Fig. 6. Effect of flowing gas type on the HDS activity of the nickel phosphides: (a) H_2 and (b) Ar.

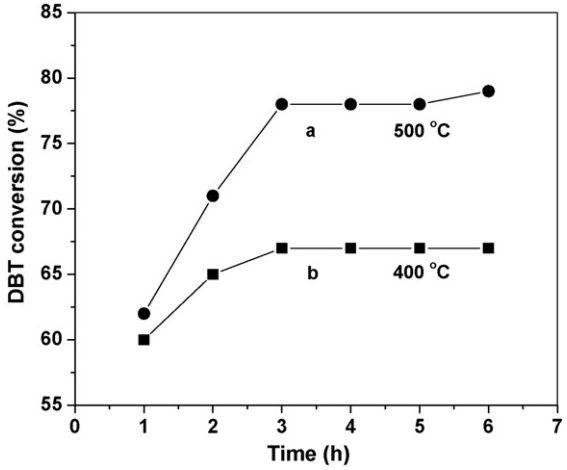

Fig. 7. Effect of reduction temperature on the HDS activity of the nickel phosphides: (a) 400 °C and (b) 500 °C.

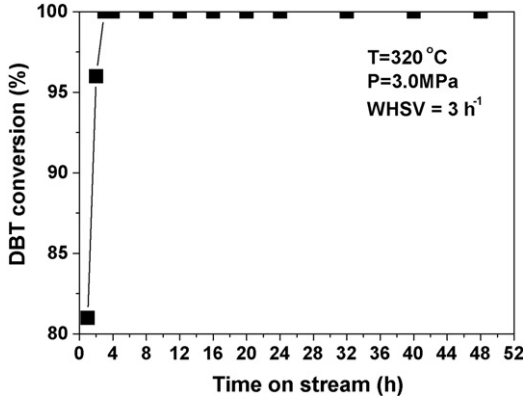

Fig. 8. Effect of reaction time on the HDS activity of the nickel phosphides.

temperature so that much more active sites of the catalysts can be exposed, leading to an improvement in the HDS performance. Fig. 8 shows the HDS results of the catalyst during 48 h. The HDS activity becomes stable within 3 h, and the HDS conversion reaches 100%. The catalyst does not suffer from deactivation during the experiment and the conversion of the final hour is still as high as 100%.

4. Conclusions

Our results demonstrate that silica–alumina-supported nickel phosphide (Ni_2P/SiO_2–Al_2O_3) was successfully prepared by the novel route proposed in the present investigation. By using metastable and nanoscale amorphous Ni–B precursors, the preparation process does not require any complex operation and high temperature. In addition, the silver-induced electroless plating was applied to synthesize the nickel phosphide catalysts, which generated an active phase that was well dispersed on the surface of the support, so that the resulting catalyst showed a high catalytic activity. The amorphous precursors can be fully phosphided above 250 °C. The as-prepared silica–alumina-supported nickel phosphide exhibited a good activity for the HDS of DBT.

Acknowledgements

The authors thank the National Natural Science Foundation of China (Grant no. 20403009), the Key Project of Chinese Ministry of Education (Grant no. 105045), and the Open Foundation of State Key Laboratory of Heavy Oil Processing at China University of Petroleum for providing financial support.

References

[1] S. Li, J.S. Lee, J. Catal. 178 (1998) 119.
[2] M. Nagai, Y. Goto, A. Miyata, M. Kiyoshi, K. Hada, K. Oshikawa, S. Omi, J. Catal. 182 (1999) 292.
[3] C. Kwak, M.Y. Kim, K. Choi, S.H. Moon, Appl. Catal. A 185 (1999) 19.
[4] B. Dhandapani, S. Ramanathan, C.C. Yu, B. Fruhberger, J.G. Chen, S.T. Oyama, J. Catal. 176 (1998) 61.
[5] J.M. Manoli, P.D. Costa, M. Brun, M. Vrinat, F. Maugé, C. Potvin, J. Catal. 221 (2004) 365.
[6] D. Ferdous, A.K. Dalai, J. Adjaye, Appl. Catal. A 260 (2004) 153.
[7] Y. Okamoto, M. Kawano, T. Kubota, Chem. Commun. (2003) 1086.
[8] Y.Q. Liu, C.G. Liu, G.H. Que, Energy Fuels 16 (2002) 3.
[9] P. Clark, W. Li, S.T. Oyama, J. Catal. 200 (2001) 140.
[10] C. Stinner, R. Prins, T. Weber, J. Catal. 202 (2001) 187.
[11] S.T. Oyama, J. Catal. 216 (2003) 343.
[12] F.X. Sun, W.C. Wu, Z.L. Wu, J. Guo, Z.B. Wei, Z.X. Jiang, F.P. Tian, C. Li, J. Catal. 228 (2004) 298.
[13] A.J. Wang, L.F. Ruan, Y. Teng, X. Li, M.H. Lu, J. Ren, Y. Wang, Y.K. Hu, J. Catal. 229 (2005) 314.
[14] X.F. Qian, X.M. Liu, Y.T. Qian, J. Solid State Chem. 149 (2000) 88.
[15] J. Park, B. Koo, K.Y. Yoon, Y.H. Wang, M. Kang, J.G. Park, T. Hyeon, J. Am. Chem. Soc. 127 (2005) 8433.
[16] C.M. Lukehart, S.B. Milne, S.R. Stock, Chem. Mater. 10 (1998) 903.
[17] W.J. Wang, H.X. Li, J.F. Deng, Appl. Catal. A 203 (2000) 293.
[18] H.X. Li, Y.D. Wu, H.S. Luo, M.H. Wang, Y.P. Xu, J. Catal. 214 (2003) 15.
[19] Y.Z. Chen, B.J. Liaw, S. Chiang, J. Appl. Catal. A 284 (2005) 97.
[20] Z. Jiang, H.W. Yang, Z. Wei, Z. Xie, W.J. Zhong, S.Q. Wei, Appl. Catal. A 279 (2005) 165.
[21] J.L. Liu, K.Y. Tao, W. Li, M.H. Zhang, P.F. Wang, L.J. Wang, Catal. Commun. 5 (2004) 301.
[22] L.J. Wang, W. Li, M.H. Zhang, K.Y. Tao, Appl. Catal. A 259 (2004) 185.
[23] Z.J. Wu, M.H. Zhang, S.H. Ge, Z.L. Zhang, W. Li, K.Y. Tao, J. Mater. Chem. 15 (2005) 4928.
[24] K. Lu, Acta Metal. Sinica 30 (1994) 1.
[25] X.W. Wang, Amorphous Materials and Application, Higher Education Press, Beijing, 1992, p. 12 (in Chinese).
[26] K. Lu, J.T. Wang, W.D. Wei, J. Appl. Phys. 69 (1991) 522.
[27] M.M. Nicolaus, H.-R. Sinning, F. Haessner, Mater. Sci. Eng. A 150 (1992) 101.
[28] H.Y. Tong, J.T. Wang, B.Z. Ding, H.G. Jiang, K. Lu, J. Non-Cryst. Sol. 150 (1992) 444.
[29] T. Spassov, U. Koster, J. Mater. Sci. 28 (1993) 2789.
[30] X.D. Liu, J.T. Wang, B.Z. Ding, Scripta Metall. Mater. 28 (1993) 59.
[31] K.F. Huo, Z. Hu, F. Chen, J.J. Fu, Y. Chen, Appl. Phys. Lett. 80 (2002) 3611.
[32] K.F. Huo, Z. Hu, J.J. Fu, H. Xu, X.Z. Wang, Y. Chen, J. Phys. Chem. B 107 (2003) 1316.
[33] S.F. Yang, C.H. Liang, R. Prins, J. Catal. 237 (2006) 118.
[34] J.Z. Cheng, Y.Z. Zhang, B.G. Zhang, Chinese Acta Sci. Nat. Univ. Nankai 34 (2001) 31.
[35] Y. Chen, Catal. Today 44 (1998) 3.
[36] JCPDS Powder Diffraction File, International Centre for Diffraction Data, Swarthmore, PA, 2002.
[37] S.J. Sawhill, K.A. Layman, D.R.V. Wyk, M.H. Engelhard, C.M. Wang, M.E. Bussell, J. Catal. 231 (2005) 300.